Chapter III

Novel roles for Ezrin in intestinal epithelial dynamics*

Abstract

Fingerlike projections called villi serve as the functional absorptive unit of the small intestine. Previous work has shown that loss of EZRIN, an apical surface protein, results in villus fusions and ectopic lumens. Initial interpretations of the EZRIN null phenotype were made with the assumption that the early intestinal epithelium is stratified and that villus domains are determined by the formation and fusion of secondary lumens. However, it is now clear that the pre-villus epithelium is a single pseudostratified layer and that villus domains are determined by patterned invaginations of the apical membrane. Re-examining the *Ezrin* null model using this revised context, we find defects in cell shape, evidence of partial stratification of the epithelium, and perturbed spindle orientation. These alterations may be directly responsible for the formation of ectopic lumens, as blebbistatin treatment of developing intestines also alters spindle angle and results in ectopic lumens. Interestingly, regardless of timing (fetal, neonatal, or adult), loss of EZRIN produces the fused villus phenotype, suggesting that a common mechanism may underlie

* This chapter represents the following manuscript in preparation for publication

Freddo AM, Wang S, Taniguchi K, Grosse AS, Gumucio DL. (2016) Novel roles for Ezrin in intestinal epithelial dynamics. In preparation.

the development of fused villi throughout life. We provide the first functional evidence for a deficit in junctional rearrangement in the absence of *Ezrin*, a mechanism that may explain the formation of villus fusions.

Introduction

The massive surface area of the small intestine, recently estimated to be about 30 square meters (Helander and Fändriks, 2014), is critical for the efficient absorption of nutrients from food. An important morphological adaptation that contributes substantially to amplification of intestinal surface area is the convolution of the epithelium into fingerlike extensions called villi. The presence of villi increases the absorptive area of the small intestine by a factor of about 6.5 times that of a flat surface (Helander and Fändriks, 2014). The critical role of villi is demonstrated in individuals with celiac disease, who suffer malabsorption concurrent with progressive loss of villi (Walker-Smith et al., 1990).

Convolution of the apical surface into villi begins at embryonic day (E)14.5 in the mouse, when villi first appear on the previously flat epithelial surface. Our understanding of the epithelial changes accompanying villus emergence has been framed by elegant morphological studies performed four decades ago (Mathan et al., 1976; Moxey and Trier, 1979). Those analyses established that before villus emergence, the intestinal epithelium is stratified and demarcation of villi occurs through the *de novo* formation of secondary lumens between the cell layers. These secondary lumens then fuse with the apical surface to form individual villus domains. Then, the surrounding epithelial cells intercalate to form a single columnar epithelium (Mathan et al., 1976).

This model was further supported by the phenotype of mice carrying the germline loss of the gene encoding EZRIN, an apical polarity protein (Saotome et al., 2004). These mice fail to thrive and contain isolated lumens throughout the intestine with minimal perturbation in overall epithelial polarity. It was concluded that this phenotype resulted from the failure of secondary lumens to fuse with the primary intestinal lumen, which prevents the stratified epithelium from becoming a simple columnar structure with individual villi (Saotome et al., 2004).

Though these early morphological studies and the *Ezrin* null mouse model make a strong case for the importance of secondary lumens in villus morphogenesis, recent studies utilizing 3D imaging techniques have established that this early intestinal epithelium is pseudostratified, not stratified, and the apical surface expands by invagination of the main lumen rather than by formation of secondary lumens (Grosse et al., 2011). In this light, the interpretation of the *Ezrin* null phenotype might be inverted. That is, rather than failure of secondary lumens to coalesce in an epithelium that is normally stratified, loss of EZRIN may lead to ectopic lumen formation and stratification of a normally single-layered structure.

Another prominent feature of the *Ezrin* null intestine is the appearance of fused villus structures; this is evident as soon as villi begin to emerge at E14.5 (Saotome et al., 2004). Interestingly, conditional loss of *Ezrin* in adult life also gives rise to fused villi (Casaletto et al., 2011). The apical surface of these mice exhibits increased active RhoA and a thickened apical actin web. Additionally, apical junctional complexes are morphologically and biochemically abnormal, leading the conclusion that the increased stability of these junctions could limit the ability of cells to separate from their neighbors as they exit the intestinal crypts and form villi, resulting in fusions. In fact, these fused villi progressively increase in complexity after EZRIN is removed. Because of the constant turnover of cells in the intestinal epithelium, this supports the

idea that these fusions are produced due to a defect in cell trafficking out of the crypt zones (Casaletto et al., 2011).

Here, we further examine several aspects of the *Ezrin* null mouse model. First, evidence is presented that loss of *Ezrin* alters the mitotic spindle angle and forms an abnormally stratified epithelium not normally observed in development. In that context, ectopic lumens can arise between cell layers. Second, the effects of conditionally deleting *Ezrin* between villus morphogenesis and crypt formation is explored; we find crypts are not required for the development of post-natal villus fusions. Third, epithelial cell dynamics was probed using the Confetti lineage tracing system.

Together, these studies provide functional evidence that the *Ezrin* null epithelium exhibits cell division and junctional dynamic deficits. These data clarify important characteristics of villus morphogenesis and demonstrate that loss of *Ezrin* results in perturbed villus architecture by a similar process in embryonic, neonatal, and adult mouse models.

Results

Conditional Ezrin loss prior to villus emergence forms ectopic lumens

To understand the effect of *Ezrin* loss both before and after villus morphogenesis, different drivers of Cre recombinase were used in combination with the *Ezrin* floxed allele (Ez^{flox}). To study the effects of *Ezrin* loss before villi form, the Ez^{flox} allele was used in combination with Cre driven by the *Shh* promoter ($Shh^{Cre\text{-}EGFP/+}$), which is active in the intestinal epithelium as early as E9.5 (Bitgood and McMahon, 1995). Immunofluorescence was used to analyze the EZRIN protein knockout efficiency of in $Ez^{flox/flox};Shh^{Cre\text{-}EGFP}$ (Ez^{ShhKO}) embryos.

In embryos harvested as early as E13.5, EZRIN protein is largely absent from the epithelium of Ez^{ShhKO} intestines (Figure III-1A-C, I-K). H&E staining of the pre-villus intestine (E13.5 and E14.5) shows that the epithelial structure is indistinguishable between control and Ez^{ShhKO} intestines (Figure III-1E-F, M-N). However, at E15.5, when the first round of villus formation is well underway, sectioned tissue reveals intraepithelial lumens and fusions between adjacent villi in Ez^{ShhKO} intestines (Figure III-1C, K). Indeed, this model closely resembles the $Ez^{-/-}$ phenotype previously reported (Saotome et al., 2004).

Analysis of the villus structures utilizing scanning electron microscopy (SEM) highlights the impaired villus architecture of the Ez^{ShhKO} intestine (Figure III-1D, L); the villi are fused to their neighbors and the overall, the villi have a slightly more rounded shape than the control villi.

Mutant villi were further analyzed at E15.5 using 3D reconstruction of confocal image z-stacks from thick (100 μm) vibratome cross-sections of intestine. This also reveals villus fusions in Ez^{ShhKO} intestines, similar to the SEM images, which are absent in wild type littermates. Additionally, in Ez^{ShhKO} mice, analysis of the apical surface reveals the presence of many ectopic lumens that are clearly disconnected from the primary intestinal lumen (Figure III-1H, P). In contrast, such disconnected lumens are never seen in control intestines; rather, all expanding lumenal surface are connected to the main lumen. Thus, the intraepithelial ectopic lumens that are observed in the absence of *Ezrin* do not result from the failure of the normal process to fully resolve, but represent ectopic structures that arise *de novo* in this mutant model.

The epithelium maintains overall apical-basal polarity after conditional loss of Ezrin prior to villus emergence

After germline *Ezrin* deletion, cell polarity in areas lacking villus fusions appears largely intact, and sorting of apical membrane proteins seems minimally altered (Saotome et al., 2004). However, since the model examined here relies on removal of *Ezrin* after polarized surfaces are already established in the gut tube, it was important to determine whether apical-basal cell polarity is altered in the *Ezrin* null intestine.

The distribution of polarity proteins in wild type and Ez^{ShhKO} intestines was compared during villus morphogenesis (E14.5 and E15.5) using apical markers aPKC (PRKCZ) and Crumbs3 (CRB3), the basolateral marker E-cadherin (CDH1), and the basal lamina marker Laminin (Figure III-2). At all times studied, overall epithelial polarity is maintained in Ez^{ShhKO} intestines and apical markers clearly reveal ectopic lumenal structures. However, as previously demonstrated, analysis of fused regions in Ez^{ShhKO} intestines revealed cells in which basolateral proteins appear to surround all surfaces (Figure III-2F, arrow), suggesting that in these regions the epithelium could be stratified.

Early loss of Ezrin results in ectopic stratification of the intestinal epithelium

Because analysis of early fused structures suggested that the epithelium might be stratified, we examined cell shape in reconstructed confocal stacks. To accomplish this the $ROSA^{mTmG/+}$ mouse model was employed. In these mice, all cells express membrane-bound Tomato fluorescent protein at baseline and express membrane-bound GFP after Cre-mediated recombination (Muzumdar et al., 2007). To maximize the number of cells that exhibit EZRIN protein loss in these experiments, a constitutive null allele of *Ezrin* (Ez^{rec}) was generated utilizing

EIIa-Cre$^{Tg/+}$ transgenic mice, in which Cre is ubiquitously expressed in the early embryo, including the germline (Lakso et al., 1996). Breeding *Ez*$^{rec/+}$*;Shh*$^{CreER/+}$ and *Ez*$^{rec/+}$*;ROSA*$^{mTmG/mTmG}$ mice allowed for generation of *Ez*$^{rec/rec}$*;Shh*$^{CreER/+}$*;ROSA*$^{mTmG/+}$ offspring. Tamoxifen was administered and E13.5 and mice were harvested at E15.5 to trace individual cells (Figure III-3A).

Analysis of mGFP expressing cells reveals that both cell shape and epithelial structure are clearly different in the *Ezrin* null background (*Ez*$^{rec/rec}$*;Shh*$^{CreER/+}$*;ROSA*$^{mTmG/+}$) compared to control (*Ez*$^{rec/+}$*;Shh*$^{CreER/+}$*;ROSA*$^{mTmG/+}$) intestines. In the control, most cells have a stereotypic tall and narrow shape and consistently contact the apical and basal surfaces via a single process (Figure III-3B-C). Nearly 90% of control cells contact both the apical and basal surfaces. Of the remaining 10%, some are undergoing mitosis and some are unable to be scored because they are located at the edge of the vibratome section (Figure III-3F). This result mirrors earlier findings, confirming that the epithelium is normally pseudostratified (Grosse et al., 2011). In contrast, in the *Ezrin* null epithelium, some cells have two distinct apical or basal processes and nearly 10% of cells have neither apical nor basal contacts (Figure III-3D-E). Additionally, only 60% of cells touch both the apical and basal surfaces, with nearly 20% contacting an ectopic lumen instead of or in addition to the primary apical surface (Figure III-3F). Together, these data confirm a substantial change in the structure of the *Ezrin* null epithelium, from a pseudostratified epithelium to one in which, at least in some regions, a stratified structure with some cells lacking apical or basal contacts.

Ezrin controls spindle angle in the early intestinal epithelium

In pseudostratified epithelia, cell division takes place at the apical surface and the plane of cell division is perpendicular to the overlying surface to allow for each daughter cell to inherit apical surface (Lee and Norden, 2013; Meyer et al., 2011). One mechanism by which a pseudostratified epithelium could become stratified is if mitotic spindles are misoriented such that cell division occurs at an oblique angle, causing one daughter to fail to inherit apical surface (Lechler and Fuchs, 2005; Lu and Johnston, 2013). EZRIN has been previously implicated in spindle angle control both in Caco2 cells *in vitro* (Hebert et al., 2012) and in the adult intestinal crypt (Casaletto et al., 2011). Thus, we examined whether the loss of EZRIN similarly perturbs spindle angle in the developing intestine. For this analysis, spindle angle was measured in dividing cells relative to the primary lumen of the intestine (Figure III-4A). A similar method was used in the zebrafish neural epithelium, which is also pseudostratified (Geldmacher-Voss et al., 2003).

It is well known that spindle angle can change until late in mitosis (Adams, 1996; Geldmacher-Voss et al., 2003). Thus, it is important to measure these angles in anaphase and telophase, when the angle of division is more stable. However, mitosis is a very rapid process, so the number of cells in these stages will be low in any single cross-section. Therefore, to aid in quantitative analysis, we used a nocodazole block and release strategy to increase the number of dividing cells. These experiments were done using an intestinal explant culture that has been previously described (Grosse et al., 2011; Walton et al., 2012; Walton et al., 2016).

Wild type or Ez^{ShhKO} intestines were harvested at E14.5, when villus formation initiates proximally, and cultured in the presence of 1 μM nocodazole, a microtubule polymerization inhibitor that irreversibly arrests cells at the G2/M transition (Figure III-4B) (Grosse et al., 2011;

Zieve et al., 1980). After six hours, a large number of arrested cells are observed in prophase (Figure III-4C). At this time, the media was exchanged to wash out the drug. Three to four hours later, intestines were harvested and spindle angles were assessed in cells in anaphase and telophase. These analyses reveal that while wild type cells divide in a plane that is nearly perpendicular to the overlying lumen, as expected, cells from Ez^{ShhKO} intestines exhibit a randomized division plane (Figure III-4D-H). Thus, in the early intestinal epithelium, as in adult intestinal crypts, EZRIN protein is an important determinant of spindle orientation.

Perturbing spindle angle is sufficient to generate ectopic lumens

Ez^{ShhKO} intestines exhibit perturbed spindle angles as well as incorrectly formed villus morphology with ectopic lumens. We next tested whether altering spindle angle using another approach would lead to ectopic lumen formation. Blebbistatin, a Myosin II inhibitor, was shown to perturb spindle angle in the zebrafish embryo during epiboly (Campinho et al., 2013). Wild type intestines were therefore treated with blebbistatin for short periods of time to determine the effect of this inhibitor on spindle angle and for longer times to assess the morphological consequences on villus development.

Intestines were harvested at E14.5 and nocodazole treatment used to synchronize the cell cycle, as above. After six hours, nocodazole was removed and intestines were further cultured in the presence of blebbistatin (5 μM) or DMSO for three to four additional hours (Figure III-5A). Though spindle angle was tightly controlled in the presence of DMSO, blebbistatin treatment resulted in a more randomized spindle angle (Figure III-5B), recapitulating the effect seen in Ez^{ShhKO} intestines (Figure III-4D).

In separate experiments, wild type intestines were harvested at E13.5 and cultured in the presence of 5 μM blebbistatin or DMSO for 48 hours. Although DMSO-treated intestines exhibit clearly demarcated villi with a continuous apical surface, blebbistatin-treated intestines exhibit ectopic lumens, similar to those seen in Ez^{ShhKO} intestines (Figure III-5C-D). These results are consistent with the idea that loss of proper spindle angle control in the early intestine can lead to formation of ectopic, isolated lumens. In the *Ezrin* null mouse, ectopic lumen formation is related to incorrect stratification of the intestinal epithelium caused by improper spindle angle.

Removal of Ezrin after villus morphogenesis results in a fused villus phenotype

Fused villi are a prominent feature in fetal and adult *Ezrin* null mice (Figure III-1) (Casaletto et al., 2011; Saotome et al., 2004). The adult phenotype was proposed to arise due to increased junctional stability and the resulting failure of cells to properly segregate from one another as they transit from the crypt to villus. If this interpretation is correct, we reasoned that inefficient cell segregation would also create fused villi in early neonatal life, when crypts have not yet formed, but cells must separate from one other as they traffic from the proliferative intervillus regions to different villi. To examine this directly, the $Villin\text{-}Cre^{Tg/+}$ driver was used in combination with $Ez^{flox/flox}$ mice. $Villin\text{-}Cre^{Tg/+}$ is active as early as E15.5 (Madison et al., 2002).

The efficiency of recombination using $Villin\text{-}Cre^{Tg/+}$ was first assessed using the $ROSA^{mTmG/+}$ reporter. By postnatal day (P)1, $Villin\text{-}Cre^{Tg/+};ROSA^{mTmG/+}$ mice show pervasive recombination in the intestinal epithelium, although rare isolated red (not recombined) cells are still present (Figure III-6A). Given the apparent efficacy of this recombination, $Ez^{flox/flox};Villin\text{-}Cre^{Tg/+}$ ($Ez^{VillinKO}$) mice were harvested at multiple time points throughout the first week of post-

natal life. While these mice initially appear grossly indistinguishable from littermate controls, by the end of the first week of life, they have failed to gain weight (Figure III-6H).

The efficiency of EZRIN loss in $Ez^{VillinKO}$ mice was assessed using immunofluorescence. At birth (P0), EZRIN loss is heterogeneous (Figure III-6B, E). At P4, some cells still retain EZRIN staining, although it is primarily restricted to villus tips (Figure III-6C, F). By P8, EZRIN is removed from the entire villus unit, from the nascent crypt base to villus tips (Figure III-6D, G). Thus, recombination at the Ez^{flox} loxP sites lags considerably behind recombination at the $ROSA^{mTmG}$ loxP sites. In addition to the progressive postnatal loss of EZRIN, a fused villus phenotype develops, mirroring the early fetal (Saotome et al., 2004) and adult (Casaletto et al., 2011) phenotypes previously characterized. These fusions increase in frequency over time (Figure III-6I), correlating with the progressive loss of EZRIN. Thus, the transition of cells out of the crypt compartment is not required to generate the fused villus phenotype. Rather, it seems likely that fused villi observed in perinatal and adult stages arise from a common mechanism.

The bizarre shapes of the fused villi in these mice give rise to regions that appear on individual sections to represent ectopic lumens. We examined these regions more carefully in confocal stacks taken from vibratome sections of intestines at P5. These analyses did not reveal any lumen that could be definitely described as isolated from the main lumen, unlike in the Ez^{ShhKO} model. Rather, all lumens examined appear to connect to the lumen in a different plane. Therefore, while we cannot rule out the possibility that some lumens may be disconnected, the vast majority of lumenal structures produced by perinatal *Ezrin* loss are contiguous with the main lumen.

Lineage tracing reveals decreased dispersion of epithelial cells in Ezrin null mice

The findings above predict that a common mechanism might underlie the development of villus fusions after loss of *Ezrin* in perinatal and adult life. The idea that junctional complexes are unusually stable, which could undermine the ability of cells to alter their contacts with neighboring epithelial cells as they separate onto different villi, is one attractive hypothesis for which there is previous evidence. Biochemical and morphological studies have revealed clear changes in junctional composition and structure after adult *Ezrin* loss (Casaletto et al., 2011); some of these same structural changes are also seen after *Ezrin* loss in the fetus (Saotome et al., 2004).

We sought to assess cell neighbor exchange in the perinatal intestine by using $ROSA^{Confetti/+}$ mice to analyze cell mixing in the presence and absence of *Ezrin*. In these mice, recombination of the $ROSA^{Confetti}$ allele turns on expression of one of four fluorescent proteins: nGFP, RFP, mCFP, and YFP (Snippert et al., 2010). We therefore generated $Ez^{VillinKO};ROSA^{Confetti/+}$ mice as well as $Ez^{flox/+};Villin\text{-}Cre^{Tg/+};ROSA^{Confetti/+}$ control mice and compared the distribution of cells of different colors at P8. This time point is around when crypts are initially established (Itzkovitz et al., 2012; Madison et al., 2002). In control mice, the epithelium is composed of dispersed cells of different colors, suggesting that epithelial cells are readily able to rearrange junctions and move away from clonally derived cells within the epithelial layer (Figure III-7A-B). However, in $Ez^{VillinKO};ROSA^{Confetti/+}$ mice, there are large blocks of a single color, indicating that cells are less readily able to rearrange junctions and separate from each other within the epithelial sheet (Figure III-7C-D).

Discussion

Several aspects of EZRIN function in the context of the fetal and perinatal intestine are revealed by these studies. First, we present evidence that loss of *Ezrin* in fetal life affects epithelial cell shape. Interestingly, studies done two decades ago suggest that EZRIN modulates cell shape in Fos-transformed fibroblasts (Lamb et al., 1997), and recent sophisticated measurements of cell mechanical properties reveal that loss of EZRIN in MDCK cells alters membrane tension, causing cells to change shape (Brückner et al., 2015). However, to our knowledge this is the first demonstration of EZRIN-dependent shape change detected in the context of a developing organ. The rounded appearance of Ez^{ShhKO} villi compared to control villi (Figure III-1J, P) provides another indication that cell membrane tension is likely altered in the *Ezrin* null epithelium. This change in villus shape has been previously noted (Saotome et al., 2004).

We also demonstrate that loss of *Ezrin* randomizes spindle angle; this phenotype had been previously seen in the intestinal crypt of *Ezrin*-deficient adult mice (Casaletto et al., 2011). However, a key aspect of this finding in fetal life is the resulting stratification of the epithelium. Though epithelial stratification was thought to be a key characteristic of the early intestinal epithelium for many years, it is now clear that the wild type intestinal epithelium is never stratified (Grosse et al., 2011). *De novo* stratification in the absence of *Ezrin*, however, may allow for the formation of ectopic lumens. Broadly, this could occur by transcytosis of apical components to create apical surfaces *de novo*, as has been described in the developing pancreatic acini (Villasenor et al., 2010) and thyroid follicles (Hick et al., 2013). Alternatively, new apical surfaces could be generated by cell division, as has been described in MDCK cells (Schlüter et al., 2009), Caco2 cells (Hebert et al., 2012; Jaffe et al., 2008), and human embryonic stem cells

(Taniguchi et al., 2015). In this case, newly stratified cells might undergo mitosis to establish a lumen deep within the epithelium.

In perinatal life, villus fusions are readily observed, but clear evidence of ectopic lumens cannot be demonstrated, suggested that their formation is directly related to the stratified phenotype described in the embryonic loss of *Ezrin*. After villi have further extended into the intestinal lumen, the epithelium only appears to be incorrectly stratified at regions that remain fused. In these regions, further lumen formation does not appear to occur, though given the complexity of these structures, cannot be fully ruled out.

Because villus fusions are observed both before crypts form and after they have developed indicates that such structures can originate from cells at the villus base, leaving open the possibility that perinatal and adult fusions develop in the same way. Functional evidence that these fusions are caused by reduced cell mixing is provided by the results of Confetti lineage tracing, which reveals large areas of contiguous color blocks in $Ez^{VillinKO}$ intestines (Figure III-7). From this and previous studies (Casaletto et al., 2011), we conclude that junctional malleability plays a key role in intestinal epithelial development and homeostasis and that the loss of *Ezrin* leads to reduced neighbor exchange as cells traffic onto the villi. Additionally, junctional stability may play a role in the distribution of cells throughout the early intestinal epithelium. Recent work from our laboratory has shown that cell division in the intestine results in non-contiguous daughter cells (Dr. Sha Wang, unpublished). Therefore, if junctions are abnormally stable in the absence of *Ezrin*, cells may be less broadly distributed after cell division. This may result in the formation of more contiguous clonal patches of cells in the intervillus regions. Once the villi have been established, such clonal patches could also produce the large contiguous blocks of color observed in the $Ez^{VillinKO}$ system.

Though the mechanism underlying the development of fusions in fetal life are still unclear, it seems very likely that a junctional defect leading to reduced cell-cell segregation could occur at this time as well. Even as the most nascent villi emerge, proliferation is restricted and compartmentalized into intervillus regions (Kolterud et al., 2009). Thus, even in these early stages, cells that are born in the proliferative intervillus zones must migrate up one of the several surrounding early villus bumps, requiring modification of their interactions with neighboring cells. This could explain the presence of villus fusions in the embryonic intestine, which are observed as soon as villi are demarcated.

Overall, this study, together with earlier work (Casaletto et al., 2011; Saotome et al., 2004), establishes that the apical protein EZRIN is required for proper villus formation and homeostasis during all stages of intestinal development. EZRIN affects multiple aspects of epithelial cell biology, including cell shape, spindle orientation, epithelial stratification, and cell-cell segregation within the epithelium.

Materials and Methods

Mice

All protocols involving mice were approved by the University of Michigan UCUCA. C57BL/6 mice were obtained from Charles River (strain 027). *Shh*$^{Cre\text{-}EGFP/+}$, *Shh*$^{CreER/+}$, *EIIa-Cre*$^{Tg/+}$, *Villin-Cre*$^{Tg/+}$, *ROSA*$^{mTmG/+}$, and *ROSA*$^{Confetti/+}$ mice were obtained from Jackson labs (Harfe et al., 2004; Lakso et al., 1996; Madison et al., 2002; Muzumdar et al., 2007; Snippert et al., 2010), and *Ez*$^{flox/flox}$ mice were obtained from Dr Andrea McClatchey (Saotome et al., 2004). Tamoxifen (Sigma) was administered to pregnant dams by gavage (250 μL of a 20 mg/mL solution dissolved in ethanol and corn oil) as described in the text.

Antibodies

Antibodies used were mouse anti-α-tubulin 1:1000 (Sigma T6199), rabbit anti-aPKC 1:250 (Santa Cruz sc-216), rabbit anti-Crumbs3 1:250 (gift of Dr Benjamin Margolis), mouse anti-Ezrin 1:1500 (Sigma E8897), mouse anti-E-cadherin 1:1000 (Invitrogen 13-1900), rabbit anti-Laminin 1:500 (Abcam ab14055), mouse anti-pHH3 1:1000 (Millipore 05-806). Secondary antibodies used were Alexa Fluor-488/555-conjugated anti-mouse and anti-rabbit 1:1000 (Invitrogen) and Alexa Fluor-568/647 Phalloidin 1:250 (Life Technologies A34055/A22287).

Tissue Immunofluorescence on Paraffin Sections

Isolated intestines were fixed overnight in 4% paraformaldehyde in PBS at 4^{o}C and then washed in PBS. After embedding in paraffin and sectioning at 5 μm, samples were deparaffinized and antigen retrieval was done in 10 mM sodium citrate before incubating with primary antibody overnight at 4^{o}C followed by secondary antibody for 30 minutes at room temperature. After mounting in Prolong Gold (Life Technologies P36930), samples were imaged on a Nikon E800 (20x objective) and a Nikon A1 Confocal (20x or 60x objective, water or oil) microscope. Image processing was done using Adobe Photoshop. Quantification was done using ImageJ.

Vibratome Sectioning and Imaging

Fixed and washed intestines were embedded in 7% (wt/vol) low-melting agarose (Sigma A9414) in PBS and sectioned at 100 μm. Samples for direct fluorescence ($ROSA^{mTmG/+}$ and $ROSA^{Confetti/+}$) were immediately mounted in Prolong Gold and imaged on a Nikon A1 Confocal microscope (20x objective, water) or Leica Upright Confocal (20x objective, water). Settings for the

ROSA^{Confetti} fluorophores were as follows (excitation, emission): mCFP (458 nm, 460-495 nm), nGFP (488, 495-515), YFP (514, 545-560), RFP (561, 580-650). Image processing was done using Imaris 8.0.

Tissue Immunofluorescence on Vibratome Sections

After blocking, primary antibody incubation was performed overnight at 4^{o}C. Secondary antibodies, along with Alexa Fluor-568 phalloidin, were incubated for 45 minutes at room temperature and then washed in PBS before mounting in Prolong Gold and imaging on a Nikon A1 Confocal microscope (20x objective, water). Image processing was done using Imaris 8.0.

Scanning Electron Microscopy

Isolated intestines were fixed at 4^{o}C in 2.5% gluteraldehyde overnight, then washed in Sorenson's phosphate buffer (0.1 M, pH 7.4). Samples were treated with hexamethyldisilazane overnight, opened utilizing a razor blade, mounted, and sputter coated with gold particle. Samples were examined on an Amray 1910 FE Scanning Electron Microscope and digitally imaged using Semicaps 2000 software. Image processing was done using Adobe Photoshop.

Intestinal Explant Culture

As reported previously (Walton and Kolterud, 2014; Walton et al., 2012), intestines were isolated from pregnant dams at E14.5 and dissected in cold DPBS (Sigma D8537). The intestines were placed on transwells (Costar 3428) in BGJb media (Invitrogen 12591-038) containing 1% penicillin-streptomycin (vol/vol) (Invitrogen 15140-122), 0.1 mg/mL ascorbic acid, and either 1 μM nocodazole (Millipore 487929), 5 μM blebbistatin (Millipore 203390) or DMSO. Intestines

were cultured for 9-48 hours at 37^{o}C with 5% CO_2. For washout experiments, intestines were washed three times with PBS before changing to media without nocodazole with or without blebbistatin.

Statistical Analysis

Performed using Prism 6 software as noted in the figure legends.

Acknowledgments

The authors would like to thank the University of Michigan Microscopy and Image Analysis Laboratory for assistance with preparing and imaging samples. The authors would like to thank Dr Elise Demitrack for assistance with the Confetti mice imaging system. We also would like to thank Dr Andrea McClatchey for mice and discussions. We also would like to thank Drs Benjamin Margolis, Linda Samuelson, Jason Spence, Daniel Teitelbaum, Kristen Verhey, Katherine Walton, and Yukiko Yamashita for discussions. Funding provided by NIH F30 DK100125 and the University of Michigan Medical Scientist Training Program (AMF) and NIH R01 DK089933 (DLG).

Author Contributions

Contributed to concepts, approaches: AMF, KT, AS, DLG

Performed experiments: AMF, SW

Analyzed data: AMF, DLG

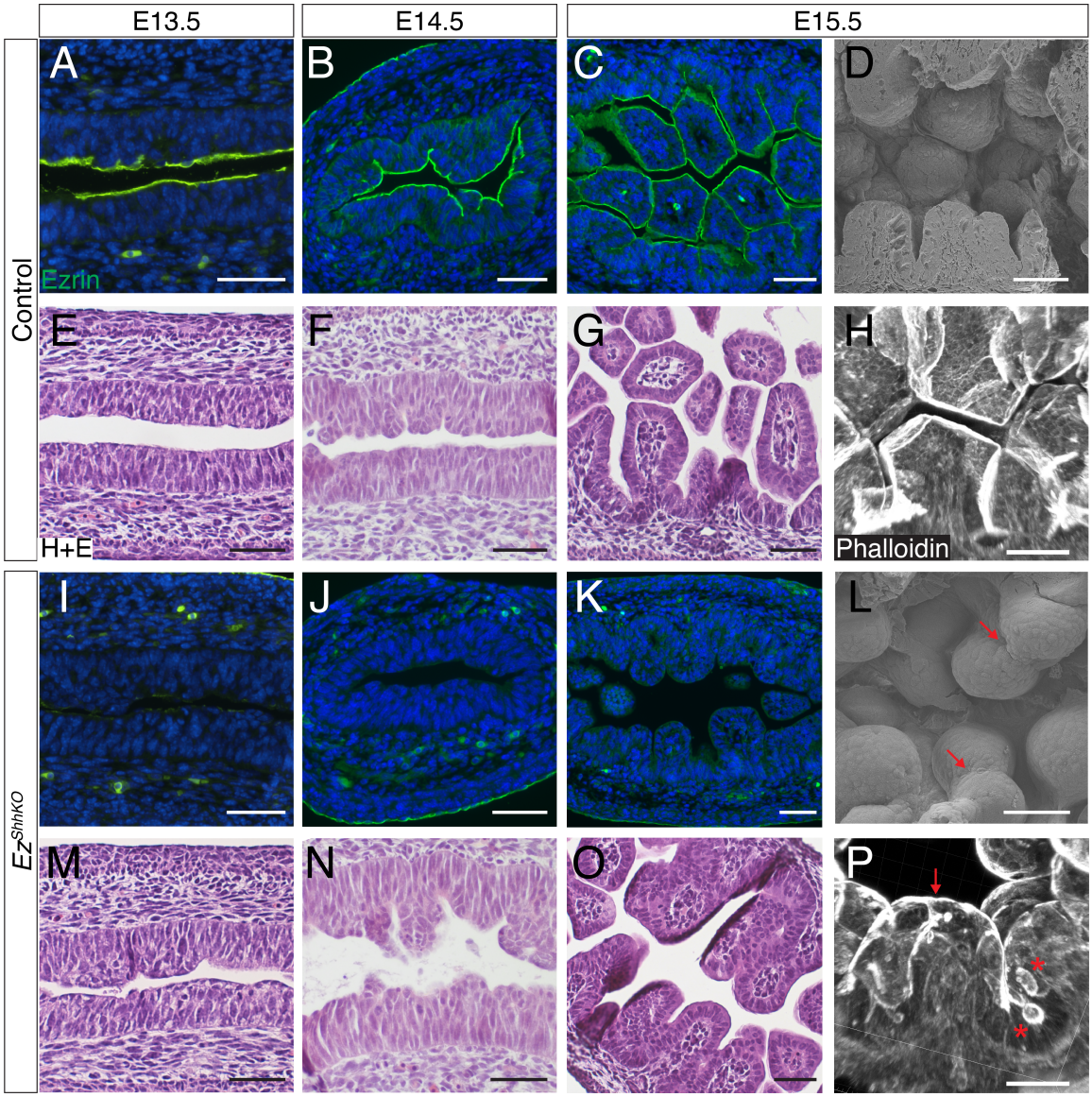

Figure III-1. *Ez*^{ShhKO} mice have villus fusions and ectopic lumens immediately after villus morphogenesis. (A-C) Control and (I-K) *Ez*^{ShhKO} intestines stained with EZRIN (green). Loss of EZRIN is observed before villus morphogenesis. (E-G, M-O) H&E stain shows the epithelial structure appears similar at (E, M) E13.5 and (F, N) E14.5. (B, O) At E15.5, villus fusions (arrows) and ectopic lumens (asterisks) are observed. These are also seen by (D, L) SEM and (H, P) 100 μm thick vibratome sections stained with phalloidin (white) (H, P). Scale bar = 50 μm.

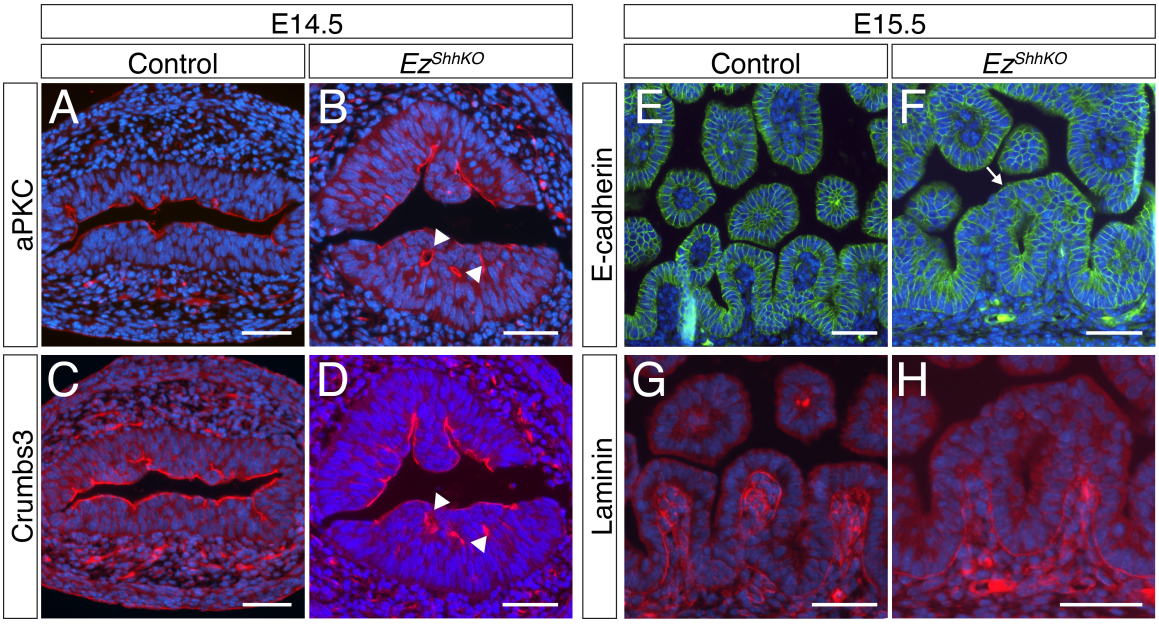

Figure III-2. Epithelial polarity is not disturbed in *Ez*^{ShhKO} intestines. (A, B) aPKC and (C, D) CRB3 are localized to the apical surfaces in these serial sections of E14.5 littermates. Ectopic lumens (arrowheads) still exhibit apical protein staining. (E, F) E-cadherin and (G, H) Laminin also are similarly distributed in control and *Ez*^{ShhKO} intestines in these serial sections of E15.5 littermates. Villus fusion (arrow) is apparent. Scale bar = 50 μm.

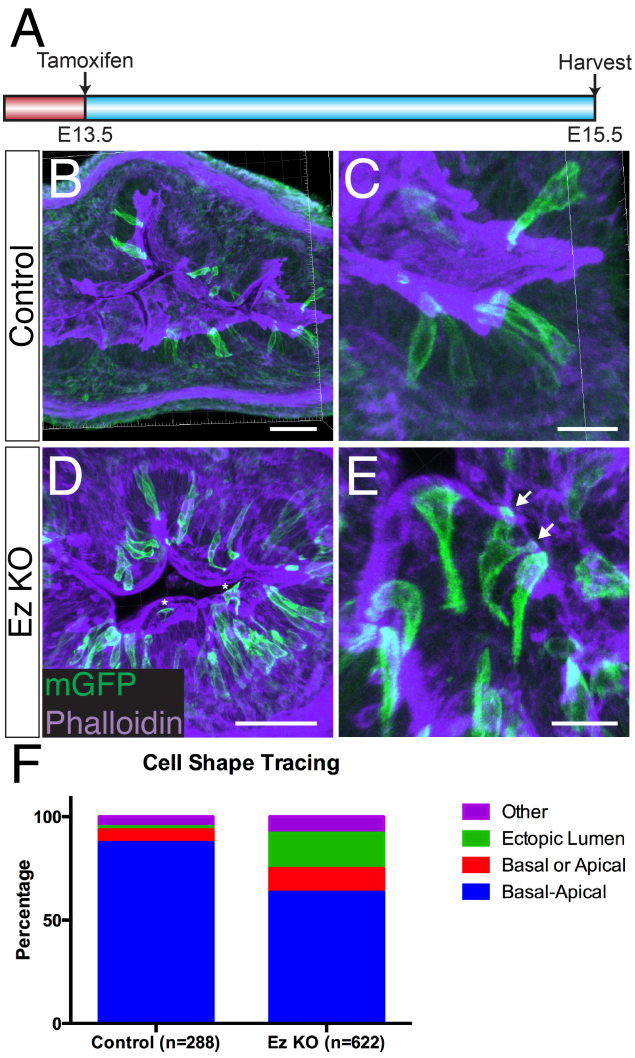

Figure III-3. *Ezrin* null intestines are partially stratified. (A) Tamoxifen dosing scheme. (B-E) Comparison of 100 μm vibratome sections of (B, C) control and (D, E) $Ez^{rec/rec};Shh^{CreER/+};ROSA^{mTmG/+}$ (Ez KO) intestines. Both labeled cells (mGFP) and apical surface (phalloidin, purple) are visualized. Some cells are disconnected from the basal surface (asterisk) or have multiple apical processes (arrows). Scale bar = 50 μm (B, D) and 20 μm (C, E). (F) Quantification of epithelial cell contacts in the control and *Ezrin* null intestines.

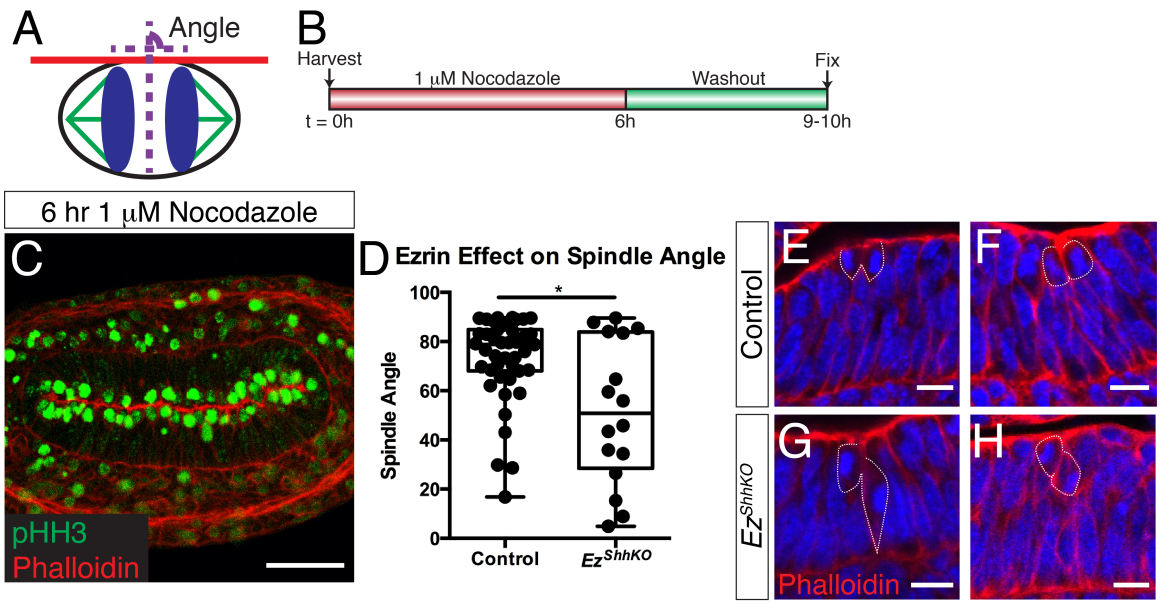

Figure III-4. Loss of *Ezrin* perturbs mitotic spindle angle. (A) Schematic of mitotic spindle angle measurements during anaphase and telophase. (B) Scheme to enrich for mitotic cells by culturing intestines in the presence of 1 μm nocodazole. (C) After 6 hours of treatment with nocodazole, a large number of mitotic cells (pHH3, green) are arrested at the apical surface (phalloidin, red) in the E14.5 intestine. Scale bar = 50 μm. (D) Quantification of spindle angle shows that loss of *Ezrin* results in a randomized spindle angle compared to control ($p < 0.05$ using Mann-Whitney test). (E-H) Cells in late anaphase and telophase in (E, F) control and (G, H) Ez^{ShhKO} intestines (outline). Note the orientation of nuclei relative to the overlying apical surface (phalloidin, red). Scale bar = 10 μm.

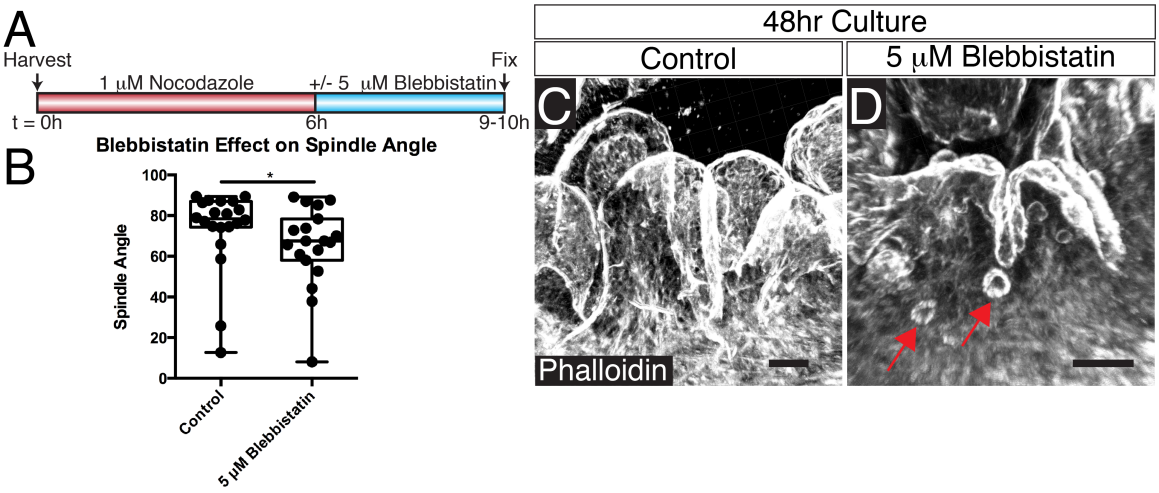

Figure III-5. Blebbistatin treatment recapitulates the *Ezrin* null phenotype. (A) Scheme for blebbistatin treatment after nocodazole block. (B) Effect of blebbistatin on spindle angle in cells in anaphase and telophase. Note the similarity of the distribution to the Ez^{ShhKO} intestines ($p < 0.05$ using Mann-Whitney test). (C, D) Culturing intestines beginning at E13.5 for 48 hours results in (C) control media results in well-demarcated villi (phalloidin, white). (D) In the presence of 5 μM blebbistatin, ectopic lumens (red arrows) are present. Compare with Ez^{ShhKO} ectopic lumens. Scale bar = 30 μm.

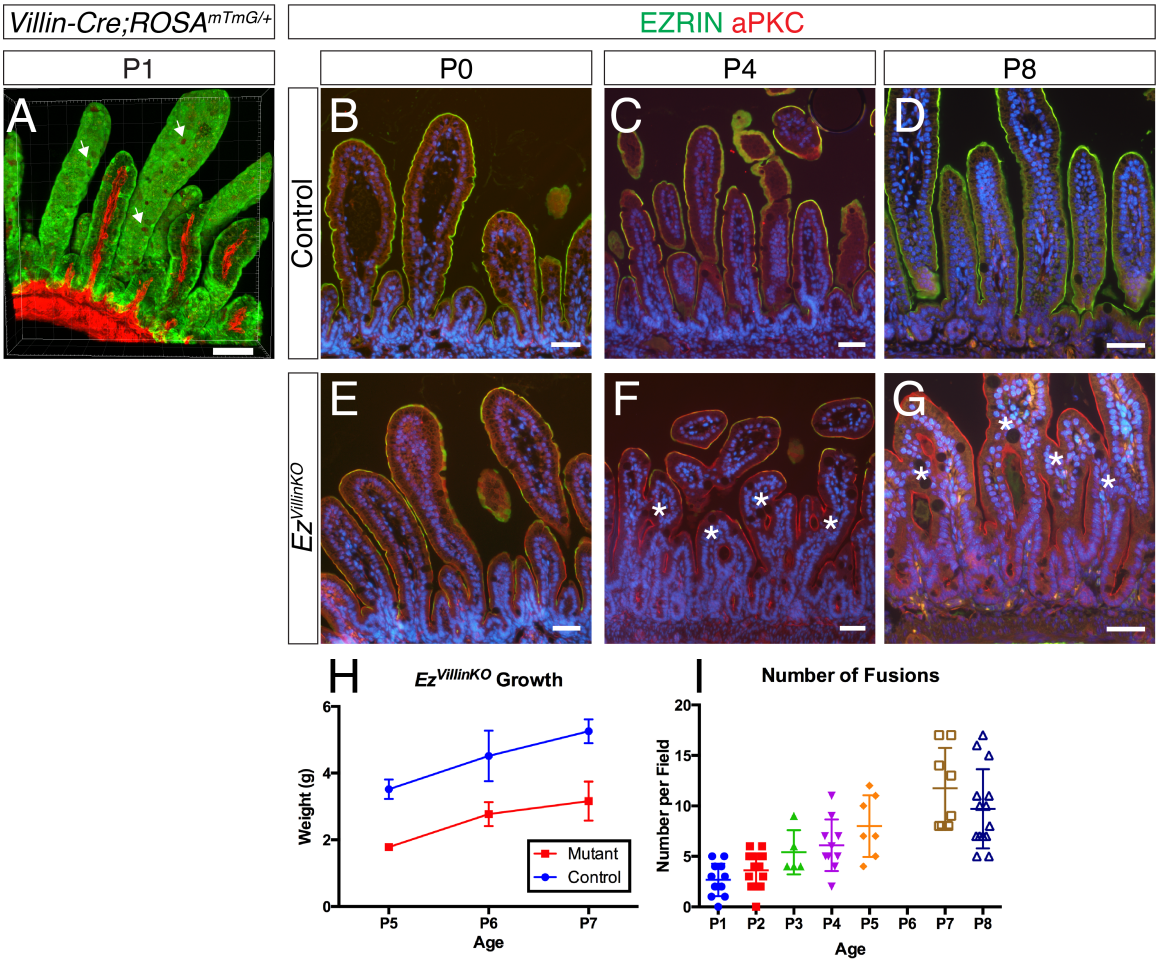

Figure III-6. Loss of *Ezrin* after villi form results in progressively more complicated villus fusions. (A) Using the *ROSA*$^{mTmG/+}$ reporter system, recombination (mGFP cells) is nearly complete at P1. Non-recombined (mRFP) cells are very rare (arrows). Scale bar = 100 μm. (B-G) Progressive loss of EZRIN (green) is observed in the first week of life. Apical surface staining (aPKC, red) reveals that villus fusions (asterisks) are increasingly complicated with increased age. Compare the (B-D) control and (E-G) *Ez*^{VillinKO} mice at (B, E) P0, (C, F) P4, and (D, G) P8. (H) Neonates fail to gain weight by the end of the first week of life. (I) Number of fusions per 10x field increases over the first week of life. Scale bar = 50 μm.

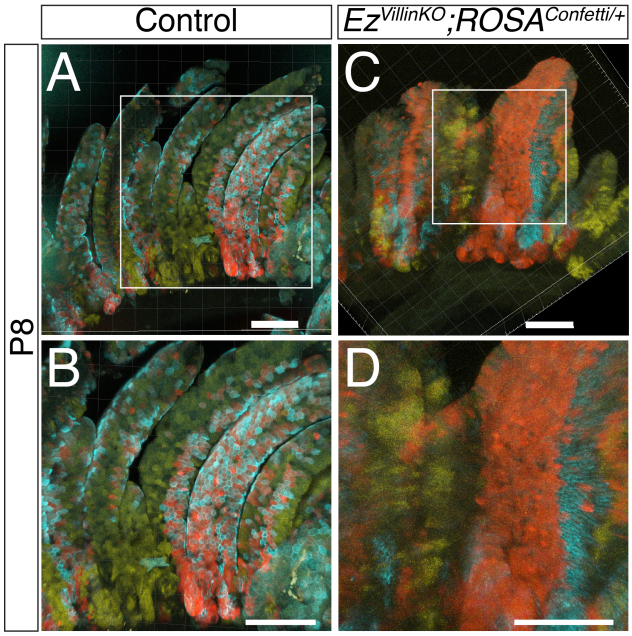

Figure III-7. Epithelial movement is restricted after neonatal loss of *Ezrin*. Comparison of (A, B) Control (*Ez*$^{flox/+}$;*Villin-Cre*$^{Tg/+}$;*ROSA*$^{Confetti/+}$) and (C, D) *Ez*^{VillinKO};*ROSA*$^{Confetti/+}$ mice at P8. Note how the colors are more interspersed in the control, while larger blocks of a single color are observed in the mutant, suggesting impaired cell junctional rearrangement. Scale bar = 100 μm.

Literature Cited

Adams, R. J. (1996). Metaphase spindles rotate in the neuroepithelium of rat cerebral cortex. *J. Neurosci.* **16**, 7610–7618.

Bitgood, M. J. and McMahon, A. P. (1995). Hedgehog and Bmp Genes Are Coexpressed at Many Diverse Sites of Cell–Cell Interaction in the Mouse Embryo. *Developmental Biology* **172**, 126–138.

Brückner, B. R., Pietuch, A., Nehls, S., Rother, J. and Janshoff, A. (2015). Ezrin is a Major Regulator of Membrane Tension in Epithelial Cells. *Scientific Reports* **5**, 14700.

Campinho, P., Behrndt, M., Ranft, J., Risler, T., Minc, N. and Heisenberg, C.-P. (2013). Tension-oriented cell divisions limit anisotropic tissue tension in epithelial spreading during zebrafish epiboly. *Nature Cell Biology* **15**, 1405–1414.

Casaletto, J. B., Saotome, I., Curto, M. and McClatchey, A. I. (2011). Ezrin-mediated apical integrity is required for intestinal homeostasis. *Proc. Natl. Acad. Sci. U.S.A.* **108**, 11924–11929.

Geldmacher-Voss, B., Reugels, A. M., Pauls, S. and Campos-Ortega, J. A. (2003). A 90-degree rotation of the mitotic spindle changes the orientation of mitoses of zebrafish neuroepithelial cells. *Development* **130**, 3767–3780.

Grosse, A. S., Pressprich, M. F., Curley, L. B., Hamilton, K. L., Margolis, B., Hildebrand, J. D. and Gumucio, D. L. (2011). Cell dynamics in fetal intestinal epithelium: implications for intestinal growth and morphogenesis. *Development* **138**, 4423–4432.

Harfe, B. D., Scherz, P. J., Nissim, S., Tian, H., McMahon, A. P. and Tabin, C. J. (2004). Evidence for an expansion-based temporal Shh gradient in specifying vertebrate digit identities. *Cell* **118**, 517–528.

Hebert, A. M., DuBoff, B., Casaletto, J. B., Gladden, A. B. and McClatchey, A. I. (2012). Merlin/ERM proteins establish cortical asymmetry and centrosome position. *Genes & Development* **26**, 2709–2723.

Helander, H. F. and Fändriks, L. (2014). Surface area of the digestive tract – revisited. *Scandinavian Journal of Gastroenterology* **49**, 681–689.

Hick, A.-C., Delmarcelle, A.-S., Bouquet, M., Klotz, S., Copetti, T., Forez, C., Van Der Smissen, P., Sonveaux, P., Collet, J.-F., Feron, O., et al. (2013). Reciprocal epithelial:endothelial paracrine interactions during thyroid development govern follicular organization and C-cells differentiation. *Developmental Biology* **381**, 227–240.

Itzkovitz, S., Blat, I. C., Jacks, T., Clevers, H. and van Oudenaarden, A. (2012). Optimality in the Development of Intestinal Crypts. *Cell* **148**, 608–619.

Jaffe, A. B., Kaji, N., Durgan, J. and Hall, A. (2008). Cdc42 controls spindle orientation to position the apical surface during epithelial morphogenesis. *The Journal of Cell Biology* **183**, 625–633.

Kolterud, A., Grosse, A. S., Zacharias, W. J., Walton, K. D., Kretovich, K. E., Madison, B. B., Waghray, M., Ferris, J. E., Hu, C., Merchant, J. L., et al. (2009). Paracrine Hedgehog Signaling in Stomach and Intestine: New Roles for Hedgehog in Gastrointestinal Patterning. *Gastroenterology* **137**, 618–628.

Lakso, M., Pichel, J. G., Gorman, J. R., Sauer, B., Okamoto, Y., Lee, E., Alt, F. W. and Westphal, H. (1996). Efficient in vivo manipulation of mouse genomic sequences at the zygote stage. *Proc. Natl. Acad. Sci. U.S.A.* **93**, 5860–5865.

Lamb, R. F., Ozanne, B. W., Roy, C., McGarry, L., Stipp, C., Mangeat, P. and Jay, D. G.

(1997). Essential functions of ezrin in maintenance of cell shape and lamellipodial extension in normal and transformed fibroblasts. *Current Biology* **7**, 682–688.

Lechler, T. and Fuchs, E. (2005). Asymmetric cell divisions promote stratification and differentiation of mammalian skin. *Nature Cell Biology* **437**, 275–280.

Lee, H. O. and Norden, C. (2013). Mechanisms controlling arrangements and movements of nuclei in pseudostratified epithelia. *Trends in Cell Biology* **23**, 141–150.

Lu, M. S. and Johnston, C. A. (2013). Molecular pathways regulating mitotic spindle orientation in animal cells. *Development* **140**, 1843–1856.

Madison, B. B., Dunbar, L., Qiao, X. T., Braunstein, K., Braunstein, E. and Gumucio, D. L. (2002). cis Elements of the Villin Gene Control Expression in Restricted Domains of the Vertical (Crypt) and Horizontal (Duodenum, Cecum) Axes of the Intestine. *Journal of Biological Chemistry* **277**, 33275–33283.

Mathan, M., Moxey, P. C. and Trier, J. S. (1976). Morphogenesis of fetal rat duodenal villi. *Am. J. Anat.* **146**, 73–92.

Meyer, E. J., Ikmi, A. and Gibson, M. C. (2011). Interkinetic Nuclear Migration Is a Broadly Conserved Feature of Cell Division in Pseudostratified Epithelia. *Current Biology* **21**, 485–491.

Moxey, P. C. and Trier, J. S. (1979). Development of villus absorptive cells in the human fetal small intestine: A morphological and morphometric study. *The Anatomical Record* **195**, 463–482.

Muzumdar, M. D., Tasic, B., Miyamichi, K., Li, L. and Luo, L. (2007). A global double-fluorescent Cre reporter mouse. *genesis* **45**, 593–605.

Saotome, I., Curto, M. and McClatchey, A. I. (2004). Ezrin is essential for epithelial organization and villus morphogenesis in the developing intestine. *Developmental Cell* **6**, 855–864.

Schlüter, M. A., Pfarr, C. S., Pieczynski, J., Whiteman, E. L., Hurd, T. W., Fan, S., Liu, C.-J. and Margolis, B. (2009). Trafficking of Crumbs3 during cytokinesis is crucial for lumen formation. *Molecular Biology of the Cell* **20**, 4652–4663.

Snippert, H. J., van der Flier, L. G., Sato, T., van Es, J. H., van den Born, M., Kroon-Veenboer, C., Barker, N., Klein, A. M., van Rheenen, J., Simons, B. D., et al. (2010). Intestinal Crypt Homeostasis Results from Neutral Competition between Symmetrically Dividing Lgr5 Stem Cells. *Cell* **143**, 134–144.

Taniguchi, K., Shao, Y., Townshend, R. F., Tsai, Y.-H., DeLong, C. J., Lopez, S. A., Gayen, S., Freddo, A. M., Chue, D. J., Thomas, D. J., et al. (2015). Lumen Formation Is an Intrinsic Property of Isolated Human Pluripotent Stem Cells. *Stem Cell Reports* **5**, 954–962.

Villasenor, A., Chong, D. C., Henkemeyer, M. and Cleaver, O. (2010). Epithelial dynamics of pancreatic branching morphogenesis. *Development* **137**, 4295–4305.

Walker-Smith, J. A., Guandalini, S., Schmitz, J., Shmerling, D. H. and Visakorpi, J. K. (1990). Revised criteria for diagnosis of coeliac disease. Report of Working Group of European Society of Paediatric Gastroenterology and Nutrition. *Archives of Disease in Childhood* **65**, 909.

Walton, K. D. and Kolterud, A. (2014). Mouse fetal whole intestine culture system for ex vivo manipulation of signaling pathways and three-dimensional live imaging of villus development. *J Vis Exp* e51817.

Walton, K. D., Kolterud, A., Czerwinski, M. J., Bell, M. J., Prakash, A., Kushwaha, J., Grosse, A. S., Schnell, S. and Gumucio, D. L. (2012). Hedgehog-responsive mesenchymal

clusters direct patterning and emergence of intestinal villi. *Proc. Natl. Acad. Sci. U.S.A.* **109**, 15817–15822.

Walton, K. D., Whidden, M., Kolterud, A., Shoffner, S. K., Czerwinski, M. J., Kushwaha, J., Parmar, N., Chandhrasekhar, D., Freddo, A. M., Schnell, S., et al. (2016). Villification in the mouse: Bmp signals control intestinal villus patterning. *Development* **143**, 427–436.

Zieve, G. W., Turnbull, D., Mullins, J. M. and McIntosh, J. R. (1980). Production of large numbers of mitotic mammalian cells by use of the reversible microtubule inhibitor nocodazole. Nocodazole accumulated mitotic cells. *Experimental Cell Research* **126**, 397–405.